PARAMETERIZATION OF WAVE RUN-UP ON BEACHES IN YUCATAN, MEXICO: A NUMERICAL STUDY

J.A. Brinkkemper[1], A. Torres-Freyermuth[2], E.T. Mendoza[2] and B.G. Ruessink[1]

Abstract

Run-up parameterization is an important tool for conducting vulnerability studies on flooding and erosion in coastal areas. This study makes use of a coupling between the SWAN and SWASH models, to investigate the influence of beach morphology and tidal water level on run-up statistics. Furthermore the applicability of current run-up parameterizations on model predictions for various beach profiles in Yucatan (Mexico) is evaluated. Results revealed that tidal water level has more influence than foreshore slope on run-up statistics. The model simulations at four different Yucatan locations showed saturation of the high frequency (f > 0.05 Hz) swash height and setup with increasing deep water wave height, whereas the infragravity swash height (f < 0.05 Hz) did not saturate for the considered conditions. The simulated 2% exceedence value was often within 25% of run-up parameterizations.

Key words: Wave run-up, swash, Yucatan, non-hydrostatic modelling, SWASH model

1. Introduction

The vulnerability of coastal areas for inundation and erosion during extreme events is dependent on both beach topography and the swash regime (Sallenger, 2000). The swash regime is described by the uprush (thin layer of water rushing up the beach) and backwash (the return flow of this thin layer), which form together the run-up. Parameterizations of run-up characteristics are an important measure in coastal vulnerability studies and have received much attention during the past two decades (e.g. Holman, 1986; Ruessink et al., 1998; Ruggiero et al., 2004; Stockdon et al., 2006; Sénéchal et al., 2011; Guza and Feddersen, 2012).

The instantaneous run-up level $\eta(t)$, is the result of a summation of the setup $\langle\eta\rangle$ (the mean water level height at the shoreline) and the swash (the variations around the mean). The run-up statistics are often related to the Irribarren number, a scale for the relative beach steepness;

$$\zeta = \frac{\beta_f}{(H_0 / L_0)^{1/2}}, \tag{1}$$

in which β_f is the foreshore slope, H_0 is the deep water wave height and L_0 is the deep water wave length. Beach conditions can be described by ζ as dissipative (ζ < 0.3), intermediate (0.3 < ζ > 1.25), and reflective (ζ > 1.25).

The significant swash height (S) is often separated into infragravity, S_{ig} (f < 0.05Hz) and incident, S_{inc} (f > 0.05Hz) swash components. Several studies have related S_{ig} and S_{inc} with β_f, H_0, L_0 or a combination of these parameters (e.g. Holman, 1986; Ruessink et al., 1998; Ruggiero et al., 2004; Stockdon et al., 2006; Sénéchal et al., 2011). Moreover, a recent numerical investigation, based on Boussinesq simulations of 2D wave propagation over planar bottom slopes, indicates an influence of frequency (f_s) and directional (σ_θ) spreading of the incoming waves on S_{ig} (Guza and Feddersen, 2012).

[1]Department of Physical Geography, Faculty of Geosciences, Institute for Marine and Atmospheric Research Utrecht, Utrecht University, Utrecht, Netherlands. j.a.brinkkemper@uu.nl, b.g.ruessink@uu.nl

[2]Instituto de Ingeniería, Laboratorio de Ingeniería y Procesos Costeros, Universidad Nacional Autónoma de México, Sisal, Yucatán, México. EMendozaP@iingen.unam.mx, ATorresF@iingen.unam.mx

For the prediction of extreme swash events, parameterizations of the 2% swash height exceedence value (R2) are often employed (Holman, 1986; Stockdon et al., 2006). Stockdon et al. (2006) derived a relationship from field observations on a wide range of beach profiles, given by:

$$R2 = 0.043(H_0 L_0)^{1/2} \tag{2}$$

$$R2 = 1.1\left(0.35\beta_f (H_0 L_0)^{1/2} + \frac{[H_0 L_0 (0.563\beta_f^2 + 0.004)]^{1/2}}{2}\right) \tag{3}$$

for $\zeta_0 < 0.3$ and $\zeta_0 > 0.3$, respectively. The foreshore slope β_f is obtained as the best fit of the beach slope in the region of $\pm 2\sigma$ of $\eta(t)$ around the mean, where σ is the standard deviation. Equation 3 is the result of the setup and swash height parameterization combined as R2 = $\langle\eta\rangle$ + S/2, in which $S = \sqrt{S_{inc}^2 + S_{ig}^2}$. In equation 3, S_{inc} and S_{ig} are represented by 0.563 β_f^2 and 0.004, respectively. The foreshore slope in the term for S_{ig} is lacking because infragravity waves are in general not breaking.

Besides the variability of run-up parameterizations in the literature, a substantial scatter of measurements around those parameterizations often exists. This variability suggests the need to further include environmental or hydrodynamic variables (i.e. tidal level, nearshore morphology, *f*s and σ_θ), which have not been accounted for in existing run-up formulations. The sole inclusion of β_f might not be enough to represent a natural beach profile. For instance, Holman and Sallenger (1985) and Guedes et al. (2011) showed the increasing influence of an offshore sandbar on run-up statistics for decreasing tidal water levels.

The aim of this work is twofold. Firstly to gain more insight on the influence of the foreshore slope and tidal water level on run-up height. Secondly to investigate the applicability of earlier published run-up parameterizations for the local beach/wave conditions in Yucatan, Mexico.

The coast of the state of Yucatan (Mexico) is prone to tropical storms (in summer) and cold front passages (in winter). The coast consists of a wide variety of beach profiles and is characterized as a low-lying coastal area, where a large part is composed of lagoons with barrier islands. Therefore, the understanding of run-up dynamics during extreme events in the study area is important for the assessment of the vulnerability to inundation. A numerical approach is chosen owing to the lack of wave and run-up measurements in the study area. Wave run-up is simulated by means of a coupling between a spectral wave model (SWAN, Booij et al., 1999) and a nonlinear non-hydrostatic model (SWASH, Zijlema et al. 2010).

2. Methods

This section describes the available information in the study area (offshore waves and beach profiles) and the numerical implementation of the simulated cases.

3.1. *Available data*

The state of Yucatan is located in the northern part of the Yucatan peninsula (Figure 1). From a geomorphological point of view, the coast presents a very mild (1:1000) wide continental shelf which extends from Celestun (east of Yucatan) to the North of the state of Quintana Roo. The tidal regime is mixed with a tidal range of 0.8 m for spring tides (Cuevas-Jiménez and Euán-Ávila, 2009).

Beach profiles were measured regularly at 26 locations (Figure 1) along the Yucatan coastline using a DGPS system. At the time of this study, 2-3 beach profiles were available for each location. The profiles near Dzilam, Hunucma, Progreso and Tizimin (Figures 1 and 2) were selected for the simulations as being representative of the morphological characteristics along the Yucatan coast. In order to allow wave run-up simulations under extreme conditions, the profiles Progreso and Dzilam were extended further landward with LIDAR information. All profiles were extended to a depth of 10 m, assuming an equilibrium profile, with the equation proposed by Dean (1977).

Wave hindcast data at 10 m water depth were available at six locations (see Figure 1). The hindcast data covered the period 1979-2008, with a temporal resolution of 15 minutes. These data were estimated with the third-generation spectral model MIKE 21SW forced by the wind re-analysis NARR (North American

Regional Reanalysis) as described by Appendini et al. (2013).
The average wave climate in Yucatan is fairly mild, with a mean wave height around 0.8 m (in 10 m water depth). However, the coast is prone to cold front passages in winter (up to 40 during the season) and tropical cyclones in summer, resulting in significant wave heights *H*s up to 3.6 m, and peak wave period *T*p=13 s. The cold front passages usually arrive from the north during the peak of the storm and generate waves with near normal wave incidence to shore. The 30-year wave hindcast information shows that the bulk of the high energetic events, which occur in the winter months, are between -30º and 30º from normal wave incidence. The mean high tidal water level is around 0.5 m higher than the mean water level; precise measurements or values for storm surge are not available.

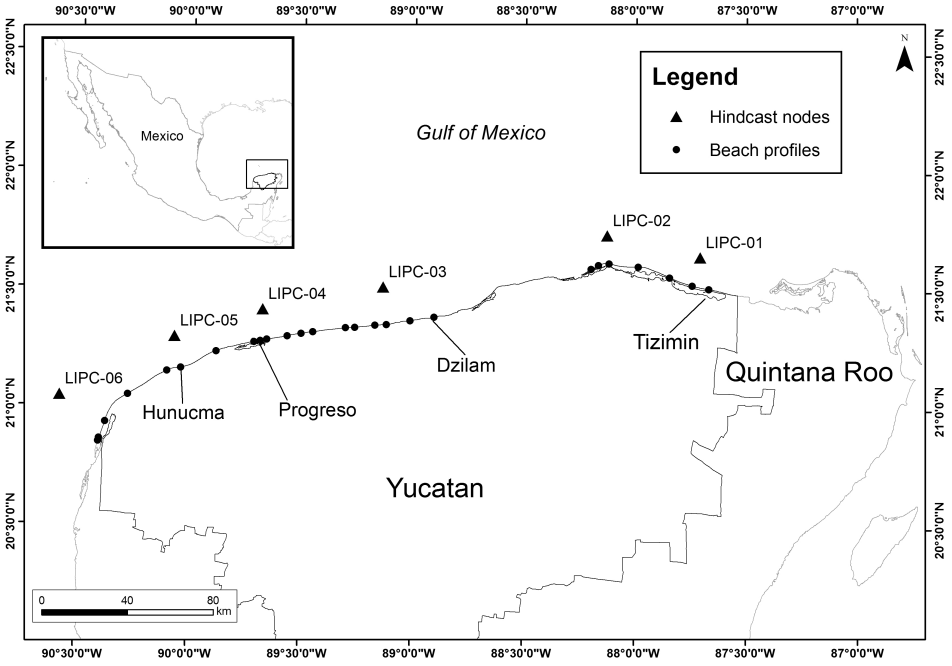

Figure 1. The study area is the coast of the state of Yucatan in the southeast of Mexico. Measured beach profiles locations (•) and the wave hindcast node locations (▲) are indicated on the map. The beach profiles used in this study are also indicated and named.

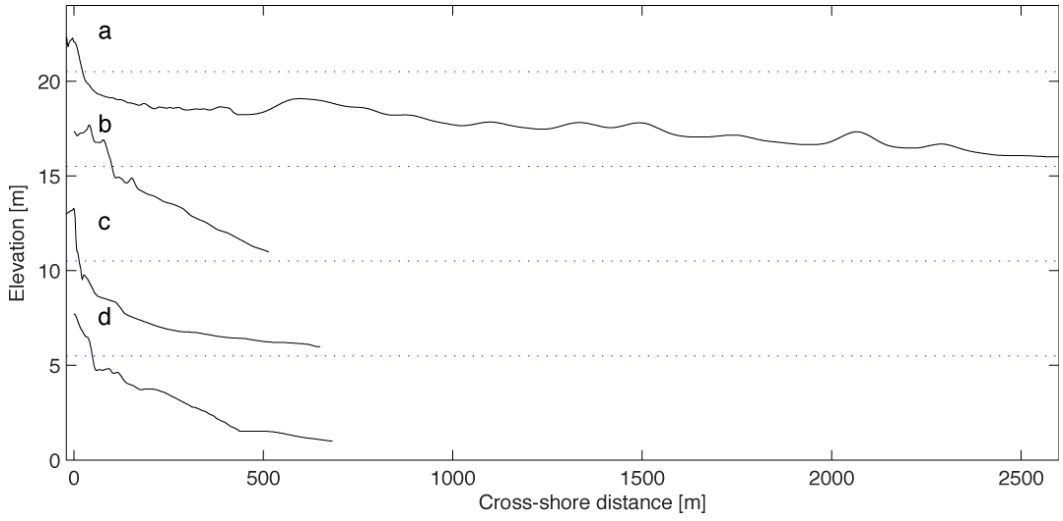

Figure 2 - Measured bottom profiles at (a) Dzilam, (b) Hunucma, (c) Progreso and (d) Tizimin to 4 m depth, used in the SWASH model simulations. The profiles are vertically spaced with 5m difference, dotted lines represent the mean water level at high tide conditions (+0.5 m).

3.2. *Model setup*

The SWAN (Booij et al., 1999) and SWASH (Zijlema et al., 2011) models were used to simulate wave propagation from 10 m water depth to the shore, including run-up, over different bottom surface profiles (Figure 2), measured along the Yucatan coastline. The SWAN model was run in stationary one-dimensional mode for the section from 10 to 4 meter water depth, with a mesh size of 1 m. The model was forced with a Jonswap spectrum, based on the wave hindcast information, at the offshore boundary. The SWAN-calculated wave energy spectrum at 4 m depth is employed as the seaward boundary for the SWASH model (Figure 3).
The SWASH domain extended from 4 m depth to the shoreline, with a one-dimensional mesh (mesh size 0.1 m) and 2 equidistant vertical layers. The initial time-step was set equal to 0.025 s and the maximum courant number to 0.5. Simulations were sampled at 5 Hz during 2170s with 5Hz, after 530s of spin up time.

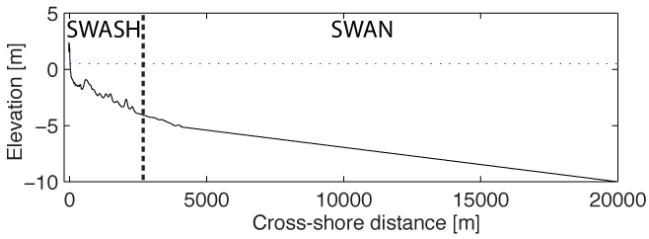

Figure 3. The simulations were performed between 10 − 4 m depth with the SWAN model, for the section from 4m till shore with the SWASH model. The Dzilam profile is used for illustration, the horizontal dotted line is the mean high tide level and the vertical dashed line represents the transition between the SWAN and SWASH simulations.

3.2.1. *Tidal water level and foreshore slope sensitivity*

For the first objective, simulations were conducted for the measured beach profile Tizimin, with different linear foreshore slopes (0.04-0.12) and different tidal water levels (0 m and +0.5 m). The bottom surface profile at Tizimin is characterized by a moderate slope with small nearshore bars, a shallow area extending ≈ 70 m from the shoreline and a steep ($\beta_f \approx 0.1$) shoreface. In order to study the influence of the foreshore slope on the run-up height, model simulations were conducted on this profile with different linear foreshore slopes (0.04-0.12), whereas the submerged profile was kept as measured below z = −0.18m (Figure 4). This resulted in a fairly natural transition. Note that z = −0.18 m was located below $\eta-2\sigma$ for all simulations, which means that β_f was equal to the slope of the linear extension. Simulations were run with the still water level at 0 m and 0.5 m, representing the mean water level and mean high tide water level in this area, respectively. The numerical model was forced using a Jonswap spectrum at 10 m water depth, for a range of shore-normal wave conditions (Hs = 1−3.2 m and Tp = 8−12 s) based on the wave hindcast information. A total of 40 simulations, four for each foreshore slope and 20 per tidal water level, were performed. The bottom friction coefficient was set spatially constant with a value of 0.002m.

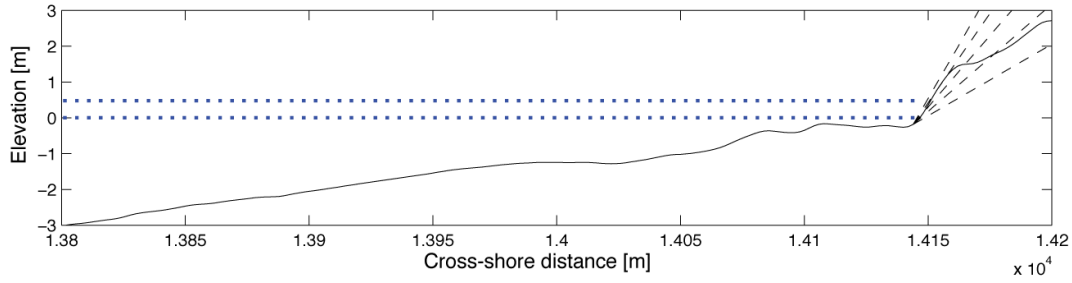

Figure 4. Beach profiles used to estimate the influence of the foreshore slope on run-up statistics at Tizimin. The solid line is the measured beach profile, whereas the dashed lines represent the different foreshore slopes (0.04, 0.06, 0.08, 0.1 and 0.12) employed in the simulations. The dotted lines represent the mean and high-tidal level (+0.5 m).

4.2.2. *Run-up parameterization for Yucatan beaches*
The second objective was to investigate the applicability of current run-up parameterizations on Yucatan beaches. Four beach profiles, named Dzilam, Hunucma, Progreso and Tizimin (Figure 2), were selected as being representative for the morphological variety in the area. The measured foreshore slopes changed spatially from 0.03 to 0.14 along the Yucatan coastline. Besides the foreshore slopes, profiles also varied in offshore slope and morphological forms such as the presence/lack of sandbars (Figure 2). The wave conditions ranged from Hs = 1 m with Tp = 7 s, up to Hs = 4 m with Tp = 12 s, realistic combinations selected from the hindcast data. A total of 18 simulations were performed, five for each profile, except for Tizimin where only 3 simulations were stable. The still water level was set to +0.5 m, representing a high tidal water level. Bottom friction coefficient was spatially constant with 0.002 m.

3.3. *Model-data analysis*

The run-up height, $\eta(t)$, was extracted from the simulations as the height of the bottom profile at the location of the wet-dry boundary in time. The wet-dry interface was tracked as the first grid point in which the water depth was zero, which corresponds to the minimum water depth used in the SWASH model (default 0.05mm). Subsequently the significant swash height (S) was calculated from the run-up height time series as:

$$S = 4\sqrt{m_0}\,, \tag{4}$$

where m_0 is the zero-th order spectral moment. The wave energy spectra are calculated with a hamming window with a length of 512s and 50% overlap, resulting in 98 degrees of freedom. Furthermore the incident (S_{inc}) and infragravity (S_{ig}) swash height were calculated by considering only the energy content at frequencies $f > 0.05$ and $f < 0.05$, respectively. The extreme run-up (R2) of the simulations was determined by sorting the run-up time series by height and extracting the 2% exceedence value.
The foreshore slope (β_f) was calculated for each case individually as the linear fit of the beach profile over the area $\langle\eta\rangle \pm 2\sigma$ of the run-up time series, following previous investigations (e.g. Ruggiero et al., 2004; Stockdon et al., 2006). This value can vary considerably for the same profile under different wave conditions (see Table 1).
Finally, the deep water wave height, H_0, was estimated for each simulation by reverse shoaling Hs, at 10 m water depth, to deep water using linear wave theory.

Table 1 –β_f range of the five bottom profiles for all simulations.

	β_f
Dzilam	0.08 - 0.09
Hunucma	0.07 - 0.08
Progreso	0.10 - 0.15
Tizimin	0.05 - 0.12

3. Results

The results of the simulated cases are presented in this section. Firstly, focus is on the run-up simulations over the Tizimin beach profile with the five different foreshore slopes, for the mean and high tidal level. Secondly, results for run-up simulations along the coast of Yucatan subject to different wave conditions are presented.

4.1. *Tidal water level and foreshore slope*

The relation between the significant swash height (S) and environmental conditions is shown by plotting S versus Hs and ζ_0 for different tidal levels (Figure 5). The swash height S is modulated by the tidal level, consistent with Holman and Sallenger (1985) and Guedes et al. (2011). Due to the gentle surfzone slope, higher water levels result in a reduction of the surf zone width and hence less wave energy is dissipated

offshore of the swash zone. The swash height increases with *H*s till saturation is reached around a value of approximately Hs = 2m, whereas a more complex dependence is observed with respect to ζ_0.

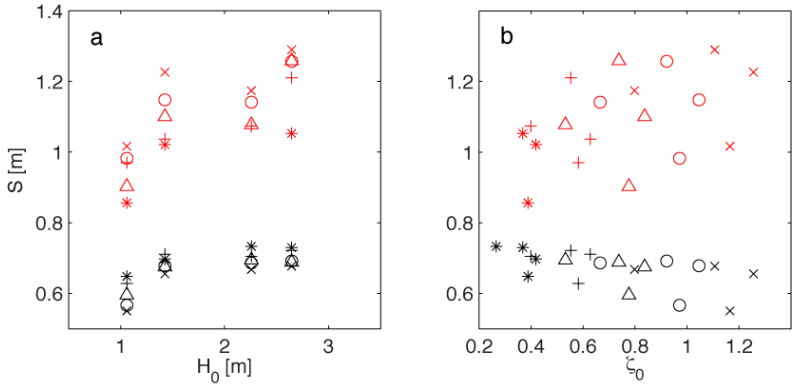

Figure 5. Predicted swash height (*S*) versus (a) deep water wave-height H_0 and (b) Irribarren number ζ_0 for the simulations with a variable foreshore slope. Black symbols represent simulations with mean water level and red symbols those with the high-tide level. Foreshore slopes were (✳) 0.04, (+) 0.06, (△) 0.08, (○) 0.10 and (×) 0.12.

To further investigate the dependence of *S* on the tidal level, the signal is split in S_{inc} and S_{ig}. The ratio between S_{inc} and S_{ig} provides a mean to identify which frequency range dominates the swash motion and increases with ζ_0 (Figure 6). For the mean water level, the surf zone width is increased with respect to the higher water level and hence the incident waves are highly dissipated. On the other hand, for high tidal level conditions the incident waves dissipate less energy in the surf zone, resulting in more incident swash energy. The predicted swash dynamics with different tidal water levels are consistent with the recent field observations in Guedes et al. (2011).
The foreshore slope also influences S_{inc}, as above dissipative slopes, high frequency waves dissipate more energy. This difference between a dissipative and a reflective slope is stronger for the high water level (Figure 5 and 6), as the water extends further landwards and covers a larger section of the attached foreshore slope. This result is also supported by the degree of incident swash energy domination for more reflective foreshore slopes (Figure 6).

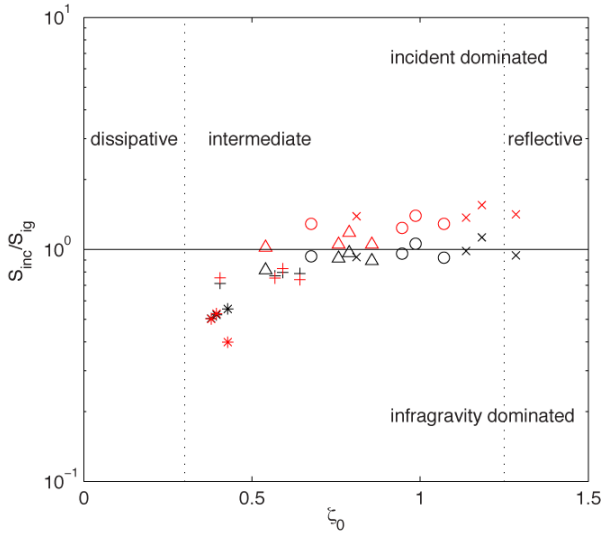

Figure 6. The ratio S_{inc}/S_{ig} versus ζ_0, for (black) mean water level and (red) high-tide level. Symbols denote the foreshore slopes (✳) 0.04, (+) 0.06, (△) 0.08, (○) 0.10 and (×) 0.12. Conditions with $\zeta_0 < 0.3$ are determined as dissipative, $0.3 < \zeta_0 < 1.25$ as intermediate and $\zeta_0 > 1.25$ as reflective.

4.2. *Run-up on Yucatan beaches*

The run-up statistics $\langle\eta\rangle$, S, S_{inc} (f > 0.05Hz) and S_{ig} (f < 0.05Hz) were calculated for each simulation as described in Section 3.3. Following previous work, linear regressions were performed for each of those statistics versus H_0, $(H_0L_0)^{1/2}$ and $\beta(H_0L_0)^{1/2}$, in order to find the best fit for the parameterizations. Linear regressions for $\langle\eta\rangle$ and S_{inc} show low correlation (r^2) and high root mean square error (rmse) with respect to simulated data (Table 2), because of the arrest in growth of S with an increase in H_0. A hyperbolic tangent fit (e.g. Sénéchal et al., 2011) through the simulations therefore result in higher r^2 and lower rmse values (Figure 7 and Table 3). S_{inc} shows saturation at H_0 > 2m (similar to the results in Figure 5a), except for the simulations at Progreso. This can be ascribed to the foreshore steepness (0.10-0.15, see Table 1) and steep surf zone slope (Figure 2) at Progreso, resulting in a low amount of incidence energy dissipation.

Table 2. Linear regression of $\langle\eta\rangle$, S_{inc} and S_{ig} versus $\beta(H_0L_0)^{1/2}$ and $(H_0L_0)^{1/2}$.

	$\beta(H_0L_0)^{1/2}$			$(H_0L_0)^{1/2}$		
	slope	r^2	rmse [m]	slope	r^2	rmse [m]
$\langle\eta\rangle$	0.24	0.47	0.52	0.02	0.50	0.50
S_{inc}	0.41	0.64	0.48	0.04	0.58	0.42
S_{ig}	0.44	0.17	0.43	0.05	0.77	0.21

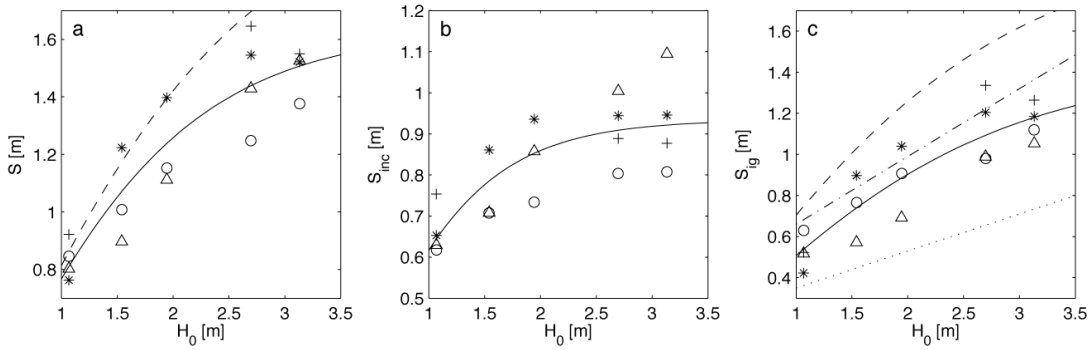

Figure 7. Predicted (a) total swash height S, (b) incident swash height S_{inc} and (c) infragravity swash height S_{ig} versus offshore significant wave height H_0, with (✳) Dzilam, (○) Hunucma, (△) Progreso and (+) Tizimin. The lines represent (-) the hyperbolic-tangent fit to the predictions (see Table 2), (- -) the hyperbolic-tangent fit of Sénéchal et al. (2011), (-.-) a linear fit to measurements by Ruggiero et al. (2004) and (...) a linear fit to measurements by Ruessink et al. (1998).

Table 3. The hyperbolic-tangent fit to swash height predictions, S = a*tanh(bH_0), see also Figure 7. The last column shows the root mean square errors in meters.

	a	b	r^2	rmse [m]
S	1.62	0.50	0.84	0.11
S_{inc}	0.93	0.78	0.61	0.08
S_{ig}	1.40	0.37	0.81	0.12

Saturation of S_{ig} with increasing H_0 is less clear than the S_{inc} saturation. The correlation coefficient and the rmse error of the linear relation $S_{ig} = 0.29H_0 + 0.25$ ($r^2 = 0.79$, rmse = 0.13 m) show no significant difference with respect to those for the hyperbolic tangent fit ($r^2 = 0.81$, rmse = 0.12 m, Table 3). Moreover, the saturation at lower frequencies was further investigated by separating these frequencies in three classes, $0.004 < f < 0.025$ Hz, $0.025 < f < 0.035$ Hz and $0.035 < f < 0.05$ Hz (Figure 8). For the three classes both a linear and hyperbolic tangent function were fit through the data. The different fits resulted in comparable r^2 for the three frequency ranges: 0.77, 0.80 and 0.79 for hyperbolic tangent fit and 0.75, 0.77 and 0.67 for the linear fit. Values for rmse for the three classes were fairly equal too. On the whole, the latter suggests that for the range of conditions simulated here, saturation was restricted to the incident wave band. This was to be expected as neither the beach slopes were very mild (as in Ruessink et al., 1998 and Ruggiero et al., 2004) or the offshore waves were very energetic (as in Senechal et al., 2011).
Linear regression for S_{ig} versus $(H_0L_0)^{1/2}$ resulted in a slope of 0.05 ($r^2 = 0.77$, rmse = 0.21 m) (Table 2), consistent to the value suggested by Senechal et al. (2011) and close to the slope of 0.06 suggested by Stockdon et al. (2006).
Finally, extreme run-up was quantified with the 2% exceedence value. The value for intermediate and reflective beaches can be parameterized as $R2 = 1.1(\langle\eta\rangle + S_{inc}+S_{ig})$. The slope of 1.1 was proposed by Stockdon et al. (2006) and was confirmed by our simulations. However, due to the shown saturation for $\langle\eta\rangle$ and S_{inc}, also simulated R2 values saturate around R2 = 1.5 m (Figure 9). The simulated R2 was higher than calculated by Stockdon et al. (2006) for low energetic conditions ($H_0 < 3$ m), but this difference decreased as H_0 increased and the predicted R2 stabilized around a value of 1.5m (Figure 9). Whether the Stockdon equation would overpredict R2 for even higher H_0 cannot be said from the current simulations.

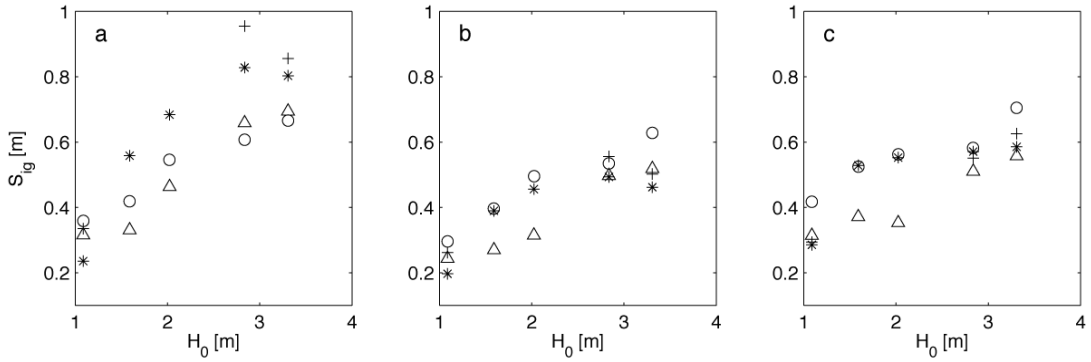

Figure 8. Infragravity swash height S_{ig} versus offshore wave height H_0 for (a) $0.004 < f < 0.025$, (b) $0.025 < f < 0.035$ and (c) $0.035 < f < 0.05$Hz. With (✳) Dzilam, (○) Hunucma, (△) Progreso and (+) Tizimin.

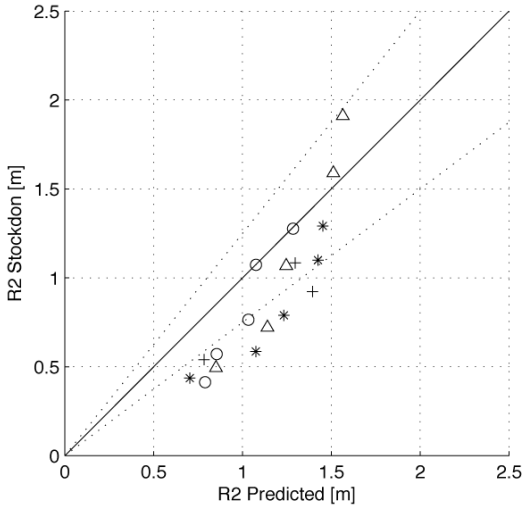

Figure 9. Parameterization of the 2% exceedence value by Stockdon et al. (2006) for the run-up simulations versus the predictions. The solid line represents the line of equality, dotted lines a 25% difference.

4. Discussion

The results suggest that a conventional linear parameterization for swash height might not be suitable for all beach profiles, given the predicted saturation of S_{inc} for offshore wave conditions. The offshore wave height at which the swash starts to saturate is site-dependent and may be one of the reasons why different parameterizations exist in the literature. It would be interesting to further investigate why and when the swash saturates as to combine existing parameterizations into a single (universal) parameterization. For lower beach slopes than the ones considered for this study, saturation is no longer limited to the high-frequency range, but may also extend into the low-frequency range. This may be the reason why the fit proposed by Ruessink et al. (1998), in which infragravity saturation was strong, underpredicts the current predicted S_{ig} (Figure 5c).
The conducted study considered modelling only cross-shore dynamics, therefore an extension to two dimensions is certainly desirable to include the effects of refraction and wave directional spread on, in particular, the infragravity swash height (Guza and Feddersen, 2012). The morphodynamic state of the measured profiles could also be an important factor to consider. The foreshore slope at a beach profile will depend on the prevailing conditions. Simulating high energetic conditions on a steep beach slope or low-energy conditions on a mild beach could result in unrealistic run-up statistics.

4. Conclusions

In this study, the effect of beach morphology and tidal level on run-up statistics at 4 locations in Yucatan (Mexico) is investigated. Simulations with two tidal water levels and a range of tide-independent foreshore slopes indicate that the tidal water level has more influence than foreshore slope on the set-up, and infragravity (f < 0.05 Hz) and incidence (f > 0.05 Hz) swash height. At all locations, the high-frequency swash height was saturated (i.e. did not increase with offshore wave conditions) for offshore wave heights exceeding about 2 m. On the other hand, the infragravity swash height did not show saturation for the wave conditions considered. The linear fit (r^2 = 0.77, rmse = 0.21 m) through the simulated S_{ig} values was equal to Senechal et al. (2011) and close to Stockdon et al. (2006). The simulated extreme run-up, defined as the 2% exceedence value, was often within 25% of the parameterization proposed by Stockdon et al. (2006) for all 4 selected beach profiles. Although for low-energetic conditions, simulated R2 values are systematic higher than predicted by the parameterization and the simulated values tend to saturate around R2 = 1.5 m.

Acknowledgements

We would like to acknowledge the role of the National Council of Science and Technology of Mexico (CONACYT) trough the FOMIX-Yucatan project (M0023-08- 06-106400) and DGAPA-UNAM (IB102012).

References

Appendini, C. M., Torres-Freyermuth, A., Oropeza, F., Salles, P., Lopez, J., Mendoza, E. T., 2013. Wave modelling performance in the Gulf of Mexico and Western Caribbean: wind reanalys assessment. *Applied Ocean Research,* 39: 20-30, doi: 10.1016/j.apor.2012.09.004

Booij, N., Ris, R. C., Holthuijsen, L. H., 1999. A third-generation wave model for coastal regions, 1. model description and validation. *Journal of Geophysical Research*, 104(C4): 7649–7666.

Cuevas-Jiménez, A., Euán-Ávila, J., 2009. Morphodynamics of carbonate beaches in the Yucatán Peninsula. Ciencias Marinas, 35(3): 307-320.

Dean, R. G. 1977. Equilibrium beach profiles: U.S. Atlantic and Gulf coasts. Departement of Civil Engineering, *Technical Report No. 12*, University of Delaware, Newark, Delaware.

Guedes, R. M. C., Bryan, K. R., Coco, G., Holman, R. A., 2011. The effects of tides on swash statistics on an intermediate beach. *Journal of Geophysical Research:* 116(C4), doi: 10.1029/2010JC006660.

Guza, R. T., Feddersen, F., 2012. Effect of wave frequency and directional spread on shoreline runup. *Geophysical Research Letters*, 39(11), L11607, doi: 10.1029/2012GL051959.

Holman, R. A., 1986. Extreme value statistics for wave run-up on a natural beach. *Coastal Engineering*, 9(6): 527-544.

Holman, R. A., Sallenger, A. H., 1985. Setup and swash on a natural beach. *Journal of Geophysical Research*, 90(C1): 945–953.

Ruessink, B. G., Kleinhans, M., van den Beukel, P., 1998. Observations of swash under highly dissipative conditions. *Journal of Geophysical Research*, 103(C2): 3111–3118.

Ruggiero, P., Holman, R., Beach, R., 2004. Wave run-up on a high-energy dissipative beach. *Journal of Geophysical Research*, 109(C06025), doi:10.1029/2003JC002160.

Sallenger, A. H., 2000. Storm impact scale for barrier islands. *Journal of Coastal Research*, 16 (3): 890–895.

Senechal, N., Coco, G., Bryan, K. R., Holman, R., 2011. Wave runup during extreme storm conditions. *Journal of Geophysical Research*, 116(C7): doi:10.1029/2010JC006819.

Stockdon, H. F., Holman, R. A., Howd, P. A., Sallenger, A. H., 2006. Empirical parameterization of setup, swash and runup. *Coastal Engineering*, 53(7): 573–588, doi: 10.1016/j.coastaleng.2005.12.005.

Thomson, J., Elgar, S., Raubenheimer, B., Herbers, T. H. C., Guza, R. T., 2006. Tidal modulation of infragravity waves via nonlinear energy losses in the surfzone. *Geophysical Research Letters*, 33(5): doi:10.1029/2005GL025514.

Zijlema, M., Stelling, G. S., Smit, P., 2011. Swash: An operational public domain code for simulating wave fields and rapidly varied flows in coastal waters. *Coastal Engineering*, 58 (10): 992–1012, doi: 10.1016/j.coastaleng.2011.05.015.